

On the Treatment of the Reference Image for InSAR Parameter Estimation for Point Scatterers

Brouwer, Wietske S.; Hanssen, Ramon F.

DOI

10.1109/IGARSS53475.2024.10641373

Publication date

Document Version Final published version

Published in

IGARSS 2024 - 2024 IEEE International Geoscience and Remote Sensing Symposium, Proceedings

Citation (APA)
Brouwer, W. S., & Hanssen, R. F. (2024). On the Treatment of the Reference Image for InSAR Parameter Estimation for Point Scatterers. In *IGARSS 2024 - 2024 IEEE International Geoscience and Remote Sensing Symposium, Proceedings* (pp. 11028-11031). (International Geoscience and Remote Sensing Symposium (IGARSS)). IEEE. https://doi.org/10.1109/IGARSS53475.2024.10641373

To cite this publication, please use the final published version (if applicable). Please check the document version above.

Copyright

Other than for strictly personal use, it is not permitted to download, forward or distribute the text or part of it, without the consent of the author(s) and/or copyright holder(s), unless the work is under an open content license such as Creative Commons.

Please contact us and provide details if you believe this document breaches copyrights. We will remove access to the work immediately and investigate your claim.

Green Open Access added to TU Delft Institutional Repository 'You share, we take care!' - Taverne project

https://www.openaccess.nl/en/you-share-we-take-care

Otherwise as indicated in the copyright section: the publisher is the copyright holder of this work and the author uses the Dutch legislation to make this work public.

ON THE TREATMENT OF THE REFERENCE IMAGE FOR INSAR PARAMETER ESTIMATION FOR POINT SCATTERERS

Wietske S. Brouwer, and Ramon F. Hanssen

Delft University of Technology, Department of Geoscience and Remote Sensing Delft, 2628 CN, The Netherlands

ABSTRACT

InSAR enables the estimation of spatio-temporal displacements, relative to a reference point and a reference epoch, here defined as the mother image. When dealing with time series, there are several options to treat the mother image in computing and plotting the temporal phase differences, producing distinctly different results, in terms of the estimated displacement parameters and their precision. Here we review the three approaches mostly encountered in literature, discuss the implications of the different approaches, and recommend the 'embracing mother' approach for standard InSAR analyses and visualizations.

Index Terms— InSAR, Point Scatterers, stochastic model, parameter estimation

1. INTRODUCTION

With InSAR (SAR Interferometry) relative displacement estimates can be obtained [1]. The primary observations obtained by the radar are used to compute a Single Look Complex (SLC) image, of which we use the phase, ψ , of reflecting objects on the Earth's surface. Since InSAR is a relative geodetic technique, and displacements can only be estimated based on phase differences, temporal Single Differences (SD) need to be computed. After the detection of coherent point scatterers, the temporal single difference phase ϕ_j^{md} for point scatterer j is the SLC phase of the daughter image relative to the phase of the mother image, i.e., $\phi_j^{md} = \psi_j^d - \psi_j^m$. Yet, since a temporal difference cannot be interpreted, we also consider the spatial difference between this point j and a reference point i. This yield a spatio-temporal double difference (DD) phase φ_{ij}^{md} , which represents the phase for point scatterer j at epoch d, relative to reference point i at mother epoch m.

Here, we evaluate how the SD phase for one single point should be defined and computed. Our evaluation covers the functional model as well as the quality description of SD, including error propagation. We discuss three approaches that primarily differ in whether the mother image is treated as a deterministic quantity or a stochastic variable. The relevance becomes apparent in subsequent stages, particularly when providing a parametric description of the displacement of individual points, e.g., in the form of an average displacement velocity. In the following sections, we discuss the three approaches for calculating the SD phases, and show how they result in a distinct quality for the computed SD phase, and thus in another quality for the estimated displacement parameters.

2. FROM A SLC PHASE TOWARDS A SINGLE TEMPORAL DIFFERENCE

The vector of SLC phase observations for point scatterer i is defined as

$$\underline{\psi}_i = [\underline{\psi}_i^m, \underline{\psi}_i^{d_1}, \underline{\psi}_i^{d_2}, \dots, \underline{\psi}_i^{d_D}]^T. \tag{1}$$

For notation convenience the mother image is defined as the first image, but it could equally be any other epoch. The stochastic model of the observations is defined as

$$Q_{\psi_i} = \begin{bmatrix} \sigma_{\psi_i^m}^2 & 0 & \dots & 0 \\ 0 & \sigma_{\psi_i^{d_1}}^2 & & \vdots \\ \vdots & & \ddots & \\ 0 & \dots & & \sigma_{\psi_i^{d_D}}^2 \end{bmatrix}, \tag{2}$$

where there is no correlation between the different SLC observations as discussed in [2].

While current InSAR time series may contain hundreds of epochs, to emphasize the effect of different approaches of computing the SD phase values, we simplified and simulated 5 daughter and 1 mother SLC values, as shown in Fig. 1. Obviously, in reality there is no trend in the SLC observations, i.e., the phase distribution is a uniform distribution between $-\pi$ and π based on the scattering mechanism only. Yet, to highlight the consequences of the different approaches it makes more sense to show the SLC observations with a trend.

¹Conventional literature frequently employs the terminology of 'master and slaves.' Here we refer to 'mother and daughters,' where the mother image is defined as the reference image.

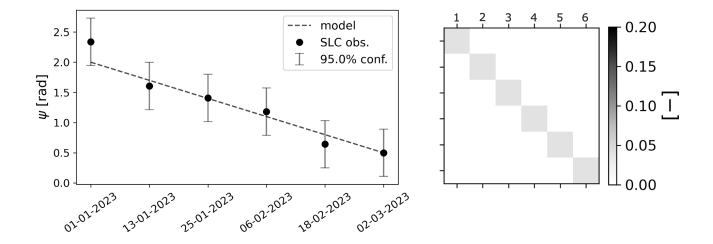


Fig. 1. Left: simulated SLC phase observations for point i with a particular trend shown by the dashed line. Right: variance-covariance matrix of the SLC phase observations. It can be seen that all observation have the same quality and that there is no correlation between the observations.

The graph of the SLC phase observations in Fig. 1 is defined as a 'position' graph, i.e., the phases are measured at a particular epoch, and the vertical axis shows the 'position' (in this case the observed phase) at a particular epoch. The horizontal axis therefore expresses time as a date.

2.1. Approach 1: Disregarding the temporal phase difference of the mother with itself ('eliminating mother')

Perhaps the most conventional approach for computing the SD values is by using the difference equation, resulting in

$$\underbrace{\begin{bmatrix} \phi_{i}^{md_{1}} \\ \phi_{i}^{md_{2}} \\ \phi_{i}^{md_{3}} \\ \vdots \\ \phi_{i}^{md_{D}} \end{bmatrix}}_{b} = \underbrace{\begin{bmatrix} -1 & 1 & 0 & \cdots & 0 \\ -1 & 0 & 1 & \cdots & 0 \\ \vdots & \vdots & \vdots & \ddots & \vdots \\ -1 & 0 & 0 & \cdots & 1 \end{bmatrix}}_{A} \underbrace{\begin{bmatrix} \psi_{i}^{m} \\ \psi_{i}^{d_{1}} \\ \psi_{i}^{d_{2}} \\ \vdots \\ \psi_{i}^{d_{D}} \end{bmatrix}}_{\psi}, \quad (3)$$

where D is the number of daughter acquisitions, as in [3, 4, 5]. Using error propagation the stochastic model for the SD phase values is computed with

$$Q_{\phi_i} = AQ_{\psi_i}A^T, \tag{4}$$

which will be a full (i.e., non-diagonal) matrix. In Fig. 2d we show the consequence of this approach, plotting the SD together with an error bar which represents the 95% confidence interval obtained from the diagonal of Q_{ϕ_i} .

The most obvious consequence of this approach is that only D SD phase values are derived from D+1 SLC phase values. In other words, the mother epoch is eliminated in the differencing operation. Consequently, plotting the obtained SD phases against absolute (calendar) dates on the horizontal axis, similar to Fig. 1, is no longer feasible, which is why we crossed out the dates. Each phase difference has to correspond to a specific time difference rather than a time. Consequently, plotting a phase difference at an epoch (or date) without explicitly stating the 'zero' point is not meaningful.

Consequently, for this approach, the results should always be plotted against a time *difference*. In contrast to the *position graph* of Fig. 1, this type of graph is referred to as a 'displacement graph.'

The modeled (simulated) trend, to be used as ground truth for comparison, is shown by the black dashed line. Subsequently, we estimate a trend and offset trough the obtained single differences, shown by the black solid line. It can be seen that the estimated trend is very similar to the simulated trend. However, comparing the 95% error bars of the SD phases with the error bars of the SLC phases we observe that the error bar of the SD phases is larger, i.e., their quality is lower. This can also be observed comparing the VCM of the SD phases, see Fig. 2a, with the VCM of the SLC phases, see Fig. 1. This is a direct result of the definition of the differencing approach, where the SLC phase vector ψ_i , is a stochastic quantity where each single observation has a particular precision. The precision of the derived SD phase is then calculated as $\sigma^2_{\phi^{md}_i} = \sigma^2_{\psi^m_i} + \sigma^2_{\psi^d_i}$, e.g., the variance of ϕ^{md}_i is the sum of the SLC phase variances of the mother and the daughter acquisition. Since the VCM shown in Fig. 2a becomes a full matrix, i.e., there is correlation between all SD phases, this implies that the complete VCM is required when estimating displacement parameters. Only using the diagonal elements of the VCM to describe the quality of the SD phases results in a too conservative quality estimation for the displacement parameters. In other words, the error bars in Fig. 2d are not sufficient to visualize the quality of the result. The gray zones in Figs. 2d-f are positioned around the adjusted observations, and indicate the 95% confidence region of these adjusted observations.

Finally, acknowledging that Fig. 2a is a displacement graph rather than a position graph implies that the interpretation of a point in the graph at time $dt = t - t_m$ is 'the displacement estimated between t and t_m ,' where t_m is the absolute date of the mother acquisition. Note that due to the differencing operation the obtained result becomes irreversible.

2.2. Approach 2: A deterministic temporal phase difference for the mother ('fixing mother')

One possibility to use a position plot with absolute dates, rather than a displacement plot, is to include the SD phase value of the mother with itself in the SD phase vector, i.e., $\phi_i^{mm} = \underline{\psi}_i^{mm} - \underline{\psi}_i^{mm} = 0 \text{ resulting in:}$

$$\underline{\phi}_i = [\phi_i^{mm}, \underline{\phi}_i^{md_1}, \underline{\phi}_i^{md_2}, \underline{\phi}_i^{md_3}, \dots, \underline{\phi}_i^{md_D}], \tag{5}$$

where $\phi_i^{mm}=0$ by definition. Note that ϕ_i^{mm} is deterministic, and in Fig. 2e it does not have an error bar. Thus, in the stochastic model, we introduce a row and column of zeros, as depicted in the VCM in Fig. 2b. Utilizing this VCM and the additional mother-mother temporal difference, we can also estimate a model through the SD phases, represented

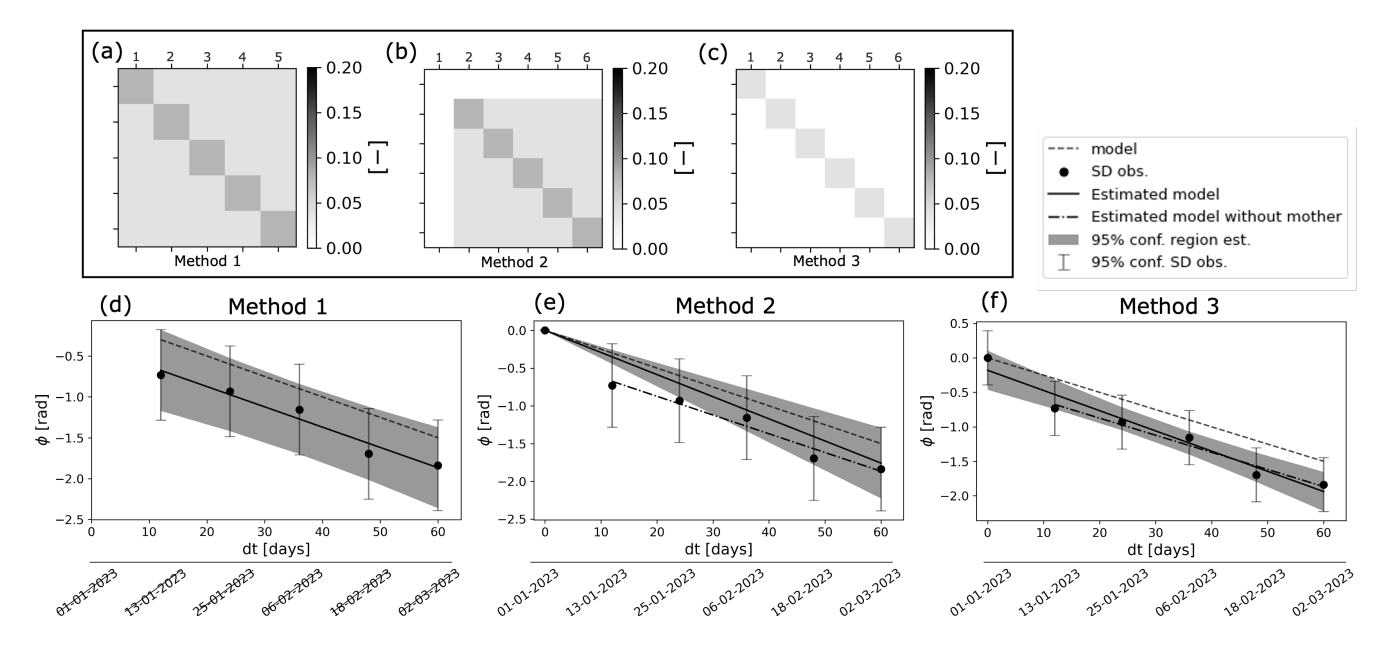


Fig. 2. In (a), (b), and (c) we show the variance-covariance matrices (VCM) of the single difference phase observations resulting from the three different approaches to compute the SD phase values. In (d), (e), and (f) the obtained single difference phase values are shown. In (d) we obtain five SD phase values, i.e., the temporal phase difference at the mother epoch is missing. Therefore the SD phases should be plotted with the delta time at the horizontal axis. In (e) the temporal phase difference at the mother epoch is added as a deterministic value, resulting in the fact that the estimated displacement model passes trough this value, resulting in an erroneous estimated model (the solid black line's slope differs from the simulated velocity shown by the dashed line). In (f) six SD phase values are obtained all being stochastic and resulting in the correct estimated velocity.

by the solid black line in Fig. 2e. As ϕ_i^{mm} is deterministic, the estimated model is constrained to pass through that value. Upon comparing the estimated model with the true simulated model (the dashed line) and the model estimated with the first approach (the dash-dotted line), it is evident that the estimated average velocity is very different from the simulated value. In fact, the trend is significantly biased by adding the deterministic SD of the mother with itself. While this bias may effectively decrease when the time series includes more epochs, this example proves that the 'fixing mother' approach is not correct. The gray zone in Fig. 2e is positioned around the adjusted observations, and indicates the 95% confidence region of these adjusted observations. This also suggests that the quality of the adjusted observations in the first part of the time series is considered to be better than the later part. Obviously, this is incorrect.

Moreover, both for approach one and two the error bars of the SD phases are greater than those of the SLC phases. A simple simulation shows that this is not to be expected. In Fig. 3 we simulate 300 complex phasors, depicted by the blue dots in (a), and computed the corresponding SLC phases, represented by the blue dots in (b), and the histogram of these SLC phases in (c). The estimated $\sigma_{\psi_i}=0.1$. Using epoch 50 as the mother acquisition, we compute the SD phasors through complex multiplication, shown by the green dots in (a). The corresponding single phase time series and histogram

were computed once again (in green). This shows that while the clutter of the SD phasors became larger, the dispersion of the SD phase values remains equivalent to that of the SLC phases, since the amplitude became larger as well due to the complex multiplication.

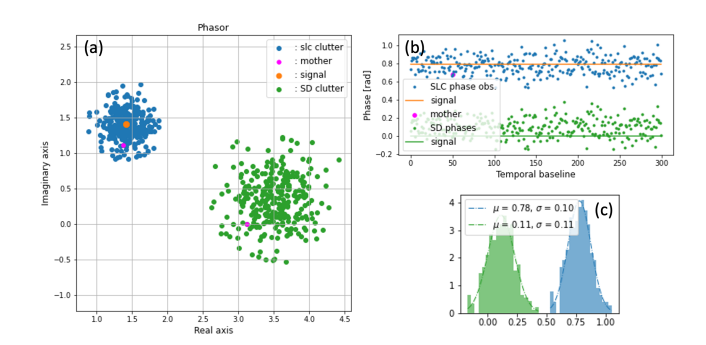


Fig. 3. (a) We simulate 300 SLC phase observations represented by the blue dots. After defining an arbitrary mother acquisition, shown by the orange dot, we compute the SD phasors (green dots). It can be seen that the phase of the mother SD phase value with itself equals zero. In (b) and (c) we show the corresponding phase values and histograms, which shows that the dispersion of the SLC phase values is equal to that of the SD values.

2.3. Approach 3: Subtracting mother realization from variates ('embracing mother')

The preferred approach to compute the SD phase values is by differencing the stochastic variates of all epochs with the deterministic realization of the mother epoch, i.e.,

$$\begin{bmatrix}
\frac{d_{i}^{mm}}{\underline{d}_{i}^{md_{1}}} \\
\underline{d}_{i}^{md_{2}} \\
\underline{d}_{i}^{md_{D}}
\end{bmatrix} = \underbrace{\begin{bmatrix}
\underline{\psi}_{i}^{m} \\
\underline{\psi}_{i}^{d_{1}} \\
\underline{\psi}_{i}^{d_{2}} \\
\underline{\psi}_{i}^{d_{D}}
\end{bmatrix}}_{\underline{\psi}_{i}} - \psi_{i}^{m}.$$
(6)

This way, with D+1 SLC phases, we retain D+1 single difference phase values since the SD phase for the mother variate, ψ , relative to its realization ψ_i is also computed.

Fig. $\overline{2f}$ is the graphical representation related to this third approach. In this case, it is a position graph. In comparison with the graphs in Figs. 2d and e, it is clear that adding the mother image appreciates and visualizes all epochs including the reference one. However, even though the single-difference phase value of the mother epoch is equal to zero, it is now stochastic, similar to all other epochs. The estimated average velocity (the solid line) is parallel to the simulated (true) average velocity, while it is not forced to pass precisely trough the temporal phase at the mother epoch as in the second approach. The gray zones in Fig. 2f is a correct representation of the quality of the adjusted observations, and indicates the 95% confidence region of these adjusted observations.

Most importantly, the distribution of the single-difference phase differences, represented by $\underline{\phi}_i$, is equivalent to that of the original SLC phases ψ_i , resulting in:

$$Q_{\phi_i} = Q_{\psi_i}. (7)$$

This equivalence is trivial, as subtracting a deterministic value from a vector of stochastic quantities should not alter the distribution of the resultant derived quantity. This is further supported through the simulations in Fig. 3. Moreover, the equivalence of Eq. (7) implies that the VCM of the single-difference vector remains a diagonal matrix, which is advantageous from a computational and visualization perspective.

3. IMPACT AND CONCLUSION

We have discussed three approaches to calculate the single differences, forming the basis of InSAR time series analysis.

The first approach, 'eliminating mother', results in (i) a visualization that lacks the presence of one of the SAR acquisition epochs, (ii) a displacement graph instead of a position graph (which implies that the information of a point in the

graph cannot be interpreted unless relative to a zero-time and a zero-displacement, and cannot contain absolute dates on the horizontal axis), and (iii) it results in a full VCM and its consequent numerical challenges. (iv) The graphical visualization of quality using error bars does not take the covariances into account, and consequently the error bars give a too conservative (pessimistic) assessment of the quality. However, the approach is mathematically valid and leads to correctly interpretable estimated parameters.

Even though it is seemingly straightforward, the second approach, 'fixing mother', can be labeled as erroneous and mathematically dubious. This is due to the fact that it results in a single-difference vector that is partly deterministic and partly stochastic. Consequently, its VCM is not full rank and therefore not invertible. This yields errors in the estimated parameters. Moreover, it does not treat all observations in an identical way.

The third approach, 'embracing mother' is regarded the preferred one, since (i) the time series visualization covers all SAR acquisitions, (ii) it can be visualized using a position graph, with calendar dates on the horizontal axis, and each point in the graph is uniquely interpretable. (iii) The approach results in a diagonal VCM for the single-differences, which is numerically advantageous, and allows for the visualization of the diagonal elements as error bars in the time series graph. Moreover, the third approach implies that the quality of the SD must be the same as the quality of the SLC values.

We conclude that the optimal way to compute temporal phase differences for a single point should be the third approach.

4. REFERENCES

- [1] R. F. Hanssen, *Radar Interferometry: Data Interpretation and Error Analysis*, Kluwer Academic Publishers, Dordrecht, 2001.
- [2] W. S. Brouwer, Y. Wang, F.J. van Leijen, and R. F. Hanssen, "On the stochastic model for InSAR single arc point scatterer time series," in *IGARSS 2023-2023 IEEE International Geoscience* and Remote Sensing Symposium. IEEE, 2023, pp. 7902–7905.
- [3] A. Ferretti, C. Prati, and F. Rocca, "Permanent scatterers in SAR interferometry," vol. 39, no. 1, pp. 8–20, Jan. 2001.
- [4] A. Ferretti, C. Prati, and F. Rocca, "Nonlinear subsidence rate estimation using permanent scatterers in differential SAR interferometry," *IEEE Transactions on geoscience and remote sens*ing, vol. 38, no. 5, pp. 2202–2212, 2000.
- [5] F. J. van Leijen, Persistent scatterer interferometry based on geodetic estimation theory, Ph.D. thesis, Delft University of Technology, Delft, the Netherlands, 2014.